Microbase Cloud Products and Associated Heating Rates in the Tropical Western Pacific

J. H. Mather and S. A. McFarlane
Pacific Northwest National Laboratory
Richland, Washington

Introduction

The microbase value added product (Miller et al. 2003) provides a standardized framework for calculating and storing continuous retrievals of cloud microphysical properties including liquid water content (LWC), ice water content (IWC), and cloud droplet size. Microbase is part of the larger broadband heating rate profile (BBHRP) project that provides a similar framework for vertical profiles of radiative heating rates. The initial development efforts for microbase and BBHRP have utilized observations from the Southern Great Plains facility. We have obtained the microbase code and have processed one month of data each for Manus (February-March 2000) and Nauru (June-July, 1999; the Nauru99 intensive operational period). The Manus period was selected because it corresponded to a period with a transition from convectively suppressed to active conditions. The Nauru99 period was chosen because of the increased frequency of sonde launches during the intensive operations period. The Nauru99 also represented one of the most convectively active at Nauru during the first several years of operation at that site.

Microbase and BBHRP are emerging as important Atmospheric Radiation Measurement (ARM) products that will provide a link to the modeling community. Current plans are to finish development of the products for the Southern Great Plains, then apply the codes to the Tropical Western Pacific (TWP) and the North Slope of Alaska. It is likely that when work on the transfer of the code to the tropics begins, modifications of the microphysical parameterizations will be required. By experimenting with these codes now, we can transfer our findings to the microbase developers to hasten the production of this data set for the TWP. At the same time, we are using the results of our calculations to characterize the tropical environment and to aid in dialogue with the tropical modeling community. Heating rates calculated from these microphysical data reveal a rich structure on a wide range of time scales. We explore various means of extracting information from these data.

Microbase and Humidity Profiles

Microbase applies simple retrievals based on ARM observations to obtain profiles of particle size, IWC, and LWC. Profiles of condensed water content (CWC = IWC + LWC) for the study periods are shown in Figures 1.

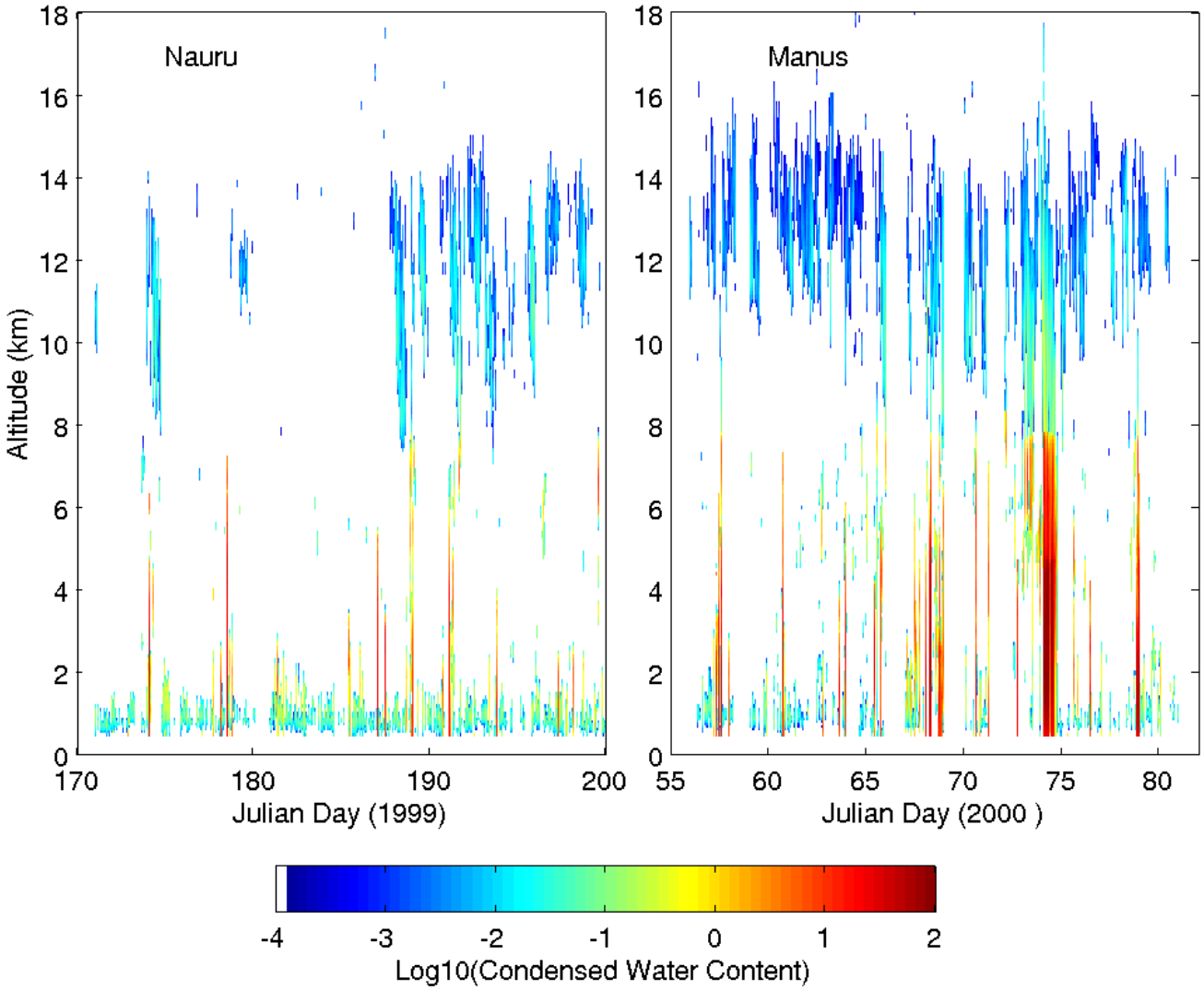

Figure 1. CWC for the Nauru 99 period, June 20 – July 20, 1999 (left panel) and for Manus, February 20 – March 20, 2000 (right panel). The color scale represents the log base 10 of the CWC in g/m^3. The retrieval breaks down in deep convection, particularly when precipitation is present. The microbase code produces instantaneous retrievals (for each radar time step) as well as 20-minute averages of these properties. For all the work described here, we have used the 20-minute averaged values.

We have adopted the standard Microbase algorithms (see Miller et al. 2003). For example, the algorithm for IWC is a power law function of radar reflectivity:

IWC = 0.097Z^^0.59 g/m^3 (Liu and Illingworth 2003).

Another way to view the CWC data is to plot the frequency distribution of the CWC as a function of height. The frequency distribution for Manus is shown in Figure 2. Plotted in this way, the data reveal a clear vertical structure. In the lowest several kilometers, a feature at low CWC values (less than 1 g/m^3)

increases approximately linearly with altitude. This shape is consistent with diluted adiabatic ascent within shallow cumulus. A second feature spanning a wide range in CWC is found near 5 km. 5 km corresponds to the freezing level and is typically a thin stable layer that can act as an impediment to deep convection. Detrainment of water is also likely at the freezing level. Clouds are frequently observed at this altitude, sometimes persisting for days. A third feature above 8 km mirrors the structure found in the shallow cumulus. Here, CWC decreases with altitude. This structure likely reflects the settling of larger particles toward the bottom and out of cirrus layers. These data have not been filtered to remove deep convection events. The feature with CWC values exceeding 10 g/m^3 below 2 km likely corresponds to these deep convective events during which the radar was attenuated by precipitation.

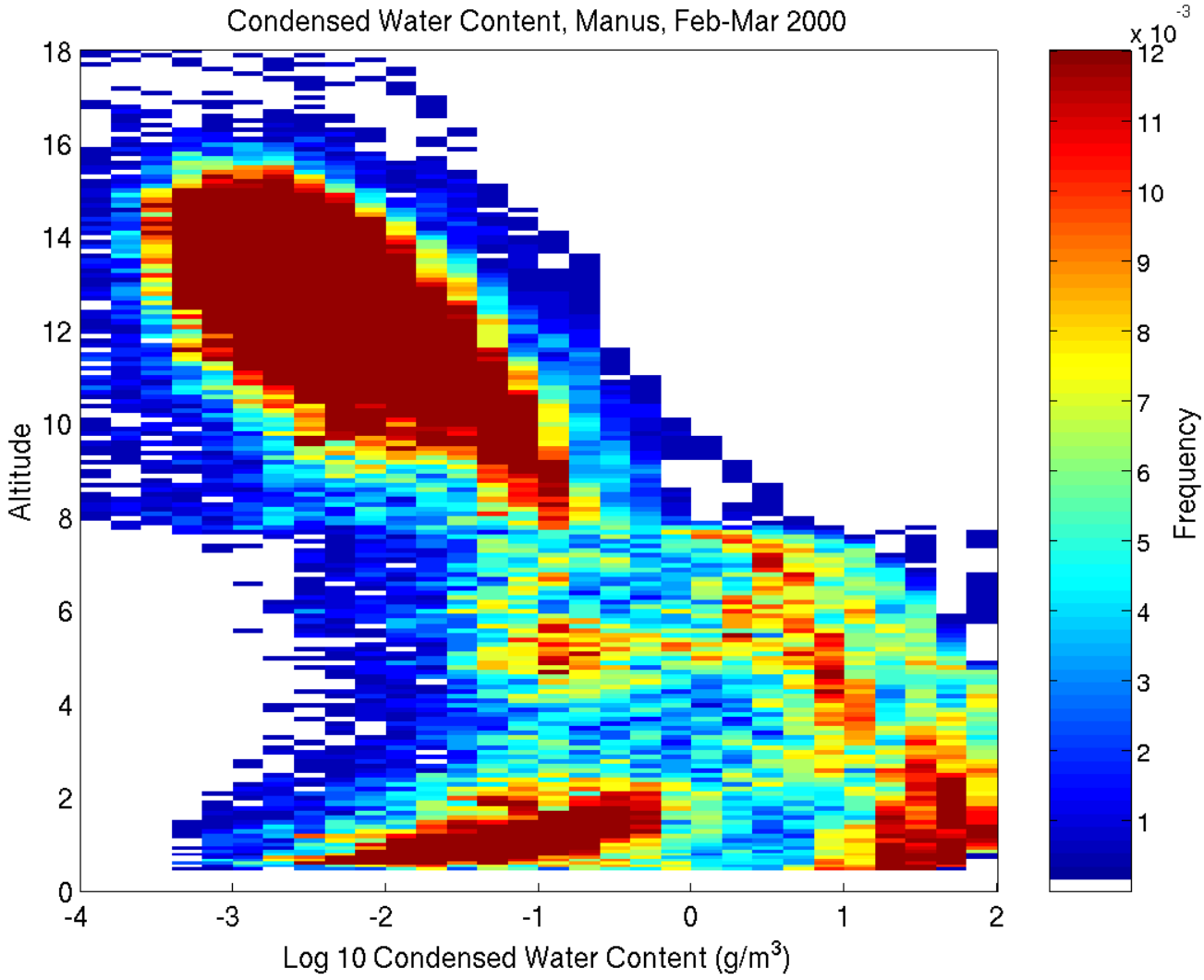

Figure 2. Frequency distribution of CWC for the Manus study period. Features can be seen associated with shallow cumulus, detrainment at the freezing level, and cirrus/anvils.

In addition to the column distribution of cloud properties, vertical profiles of temperature and water vapor content are also needed to calculate radiative flux profiles and heating rates. These thermodynamic profiles are needed on a time grid consistent with the cloud properties, in this case, 20-minute intervals. We have derived a thermodynamic product from radiosondes in which the column water is constrained by water vapor column amounts derived from the microwave radiometer (MWR). After experimenting with several techniques, we adopted the following set of procedures for deriving the high temporal resolution thermodynamic product:

1. Remove MWR water vapor outliers
2. Smooth MWR vapor and interpolate to 20 minute grid
3. Scale sonde profiles to MWR vapor
4. Linearly interpolate sonde profiles to six hour temporal grid
5. Iteratively scale interpolated sondes to MWR water (see below)
6. Linearly interpolate scaled sondes to final 20-minute resolution

During much of the Nauru 99 experiment, sondes were launched four times daily. Outside of this experiment, twice-daily launches are standard. When sondes are launched less than four times per day, the column water interpolated from the sonde profiles can differ greatly from the MWR values, particularly at times well away from the sonde launch. The interpolation of sondes to 6-hour intervals and the subsequent iterative scaling was an attempt to produce a thermodynamic time series that was consistent with the MWR, preserved the structure near sonde launches, and was physically reasonable throughout the column. The main concern on this last point was to avoid high values of supersaturation with respect to water. To avoid this problem, rather than simply scaling the sonde water to the MWR, when the sonde was dry relative to the MWR, the relative humidity (RH) was gradually increased by a uniform fraction of 100-RH(z) where RH(z) is the RH as a function of height. Thus, if RH = 100% at some altitude, the RH is not increased. In this way, the general shape of the water vapor profile is preserved. The 20-minute RH data for Nauru are shown in Figure 3.

Calculation of Radiative Fluxes and Heating Rates

The broadband fluxes and heating rates are calculated using the spherical harmonics discrete ordinates method (SHDOM) radiative transfer model in one-dimensional mode. Gaseous absorption is treated with correlated k-distributions derived from the rapid radiative transfer model (RRTM). The correlated k-distribution has 13 bands in the shortwave and 15 bands in the longwave, covering the wavelength range from 0.2 to 1000 um. The absorption coefficients are provided by the line-by-line radiative transfer model and based on the 1992 high-resolution transmission parameter database and the CKD-2.2 water vapor continuum model (Mlawer et al. 1997).

Optical properties of liquid water clouds are calculated from Mie theory. In the shortwave, single scattering properties of ice crystals are obtained from the calculations of Yang et al. 2000. Bulk scattering properties are obtained by integrating the single scattering properties over a gamma size distribution with a given effective radius and IWC. In the longwave, ice cloud scattering properties are calculated from Mie theory assuming distributions of spheres with volume/area ratios equivalent to the volume/area ratios of the crystals used in the shortwave calculations.

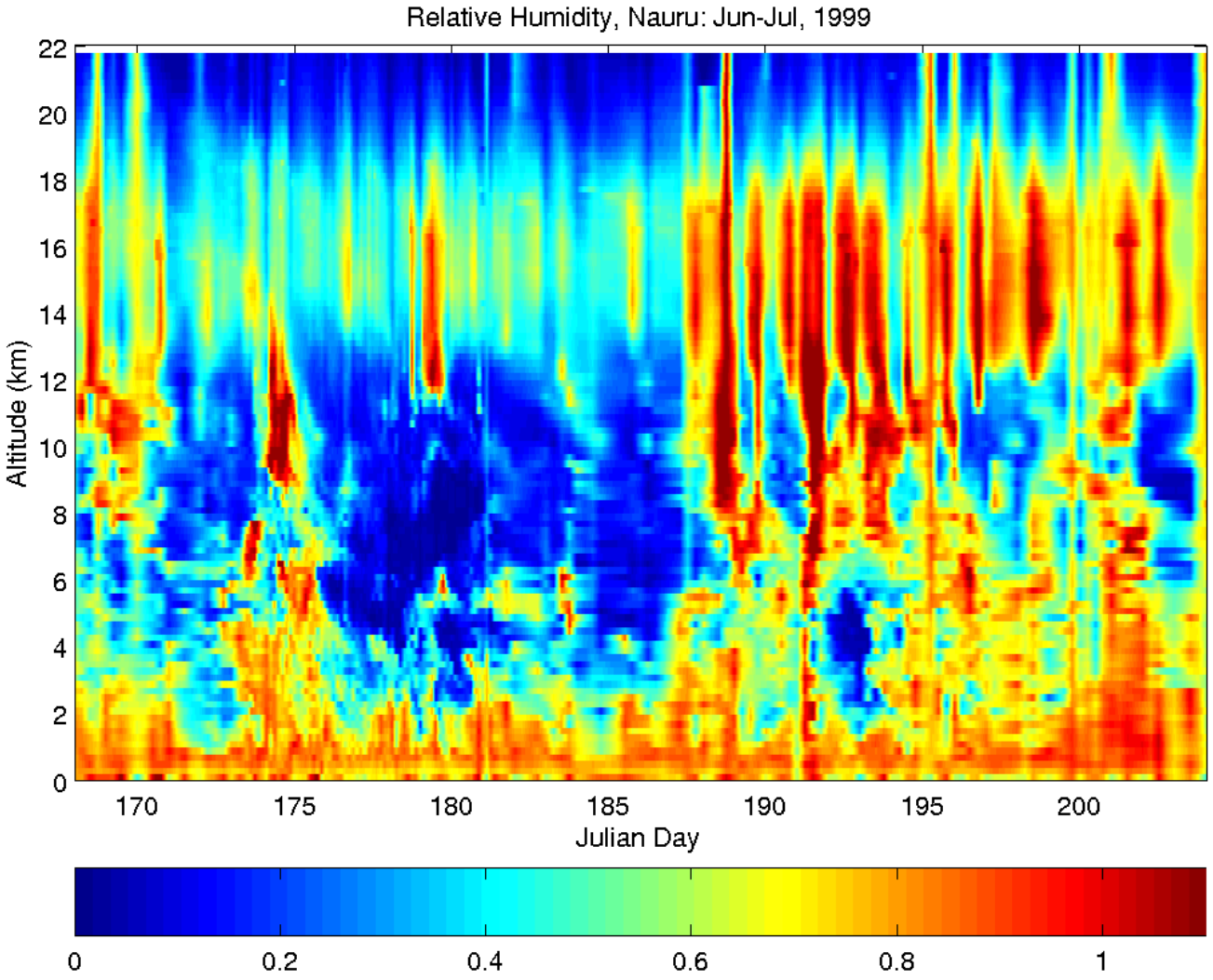

Figure 3. Interpolated RH profiles for the Nauru 99 period

For both Manus and Nauru, radiative fluxes were calculated at 20-minute intervals throughout the vertical column. From these flux profiles, heating rates (reported in units of K/day) were calculated. Three separate sets of calculations were done for each site. First, fluxes were calculated with no clouds included. This clear sky calculation provides a baseline to allow the radiative impact of the clouds to be identified. Second, a calculation was done with only boundary layer clouds removed. Boundary layer clouds tend to be highly variable in time. To minimize the impact of averaging, fluxes were calculated with and without these boundary layer clouds. The temporal cloud fraction is provided in the microbase files. This cloud fraction was used to combine the two sets of cloud fluxes into a flux product that best represents an average over the 20-minute period. Figure 4 shows the radiative heating (the final cloud product with averaging of the boundary layer fluxes) rate profiles for Nauru. The diurnal cycle and the influence of clouds are both evident in this figure. The heating rate scale was constrained to be quite narrow to illustrate variability due to water vapor as well as clouds. Instantaneous heating and cooling rates associated with clouds often exceed 10 K/day (Ackerman et al. 1988).

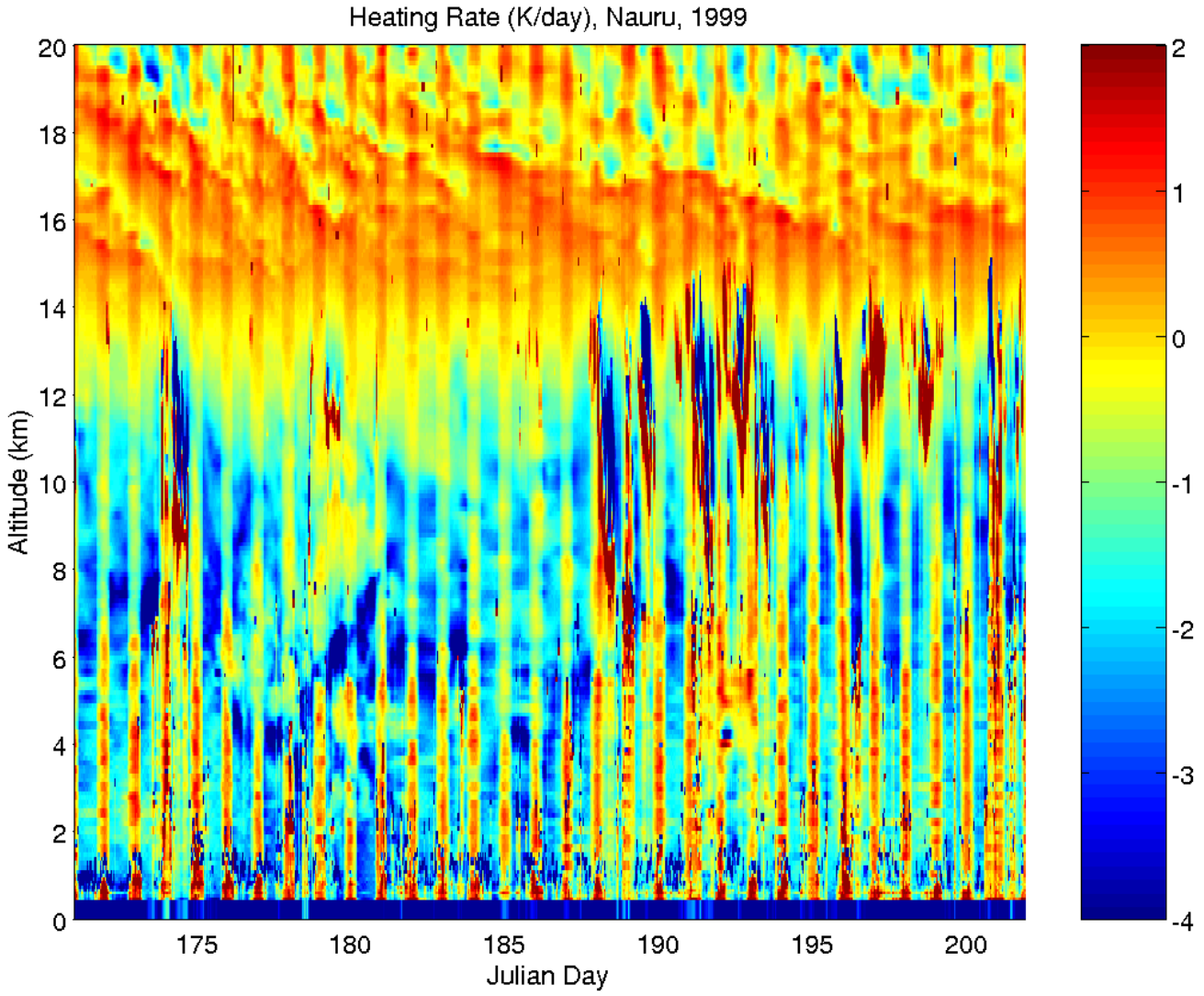

Figure 4. Heating rate profiles calculated for the Nauru 99 period. The heating rate reflects heating due to both longwave and shortwave flux convergence. Positive values indicate heating while negative values indicate cooling.

To assess the reasonableness of our results, we have compared the calculated fluxes with fluxes observed at the surface and at the top of atmosphere. The surface fluxes were obtained from the TWP ARM sites, while top of atmosphere fluxes were derived from geostationary satellite data (Nordeen et al. 2001). Longwave flux comparisons for the surface and top of atmosphere are shown in Figure 5. For the top of atmosphere comparison, the calculated fluxes tend to fall below those derived from the geostationary satellite observations while at the surface; the calculated fluxes are higher than observed values. In both cases, the discrepancies are consistent with an overestimate of the cloud optical depth. In the future, we will explore other microphysics parameterizations to determine which schemes provide the best agreement with the column boundary fluxes and to determine the uncertainties in fluxes and heating rates resulting in the uncertainties in the cloud microphysical properties. For this work, we will use the standard microbase retrievals.

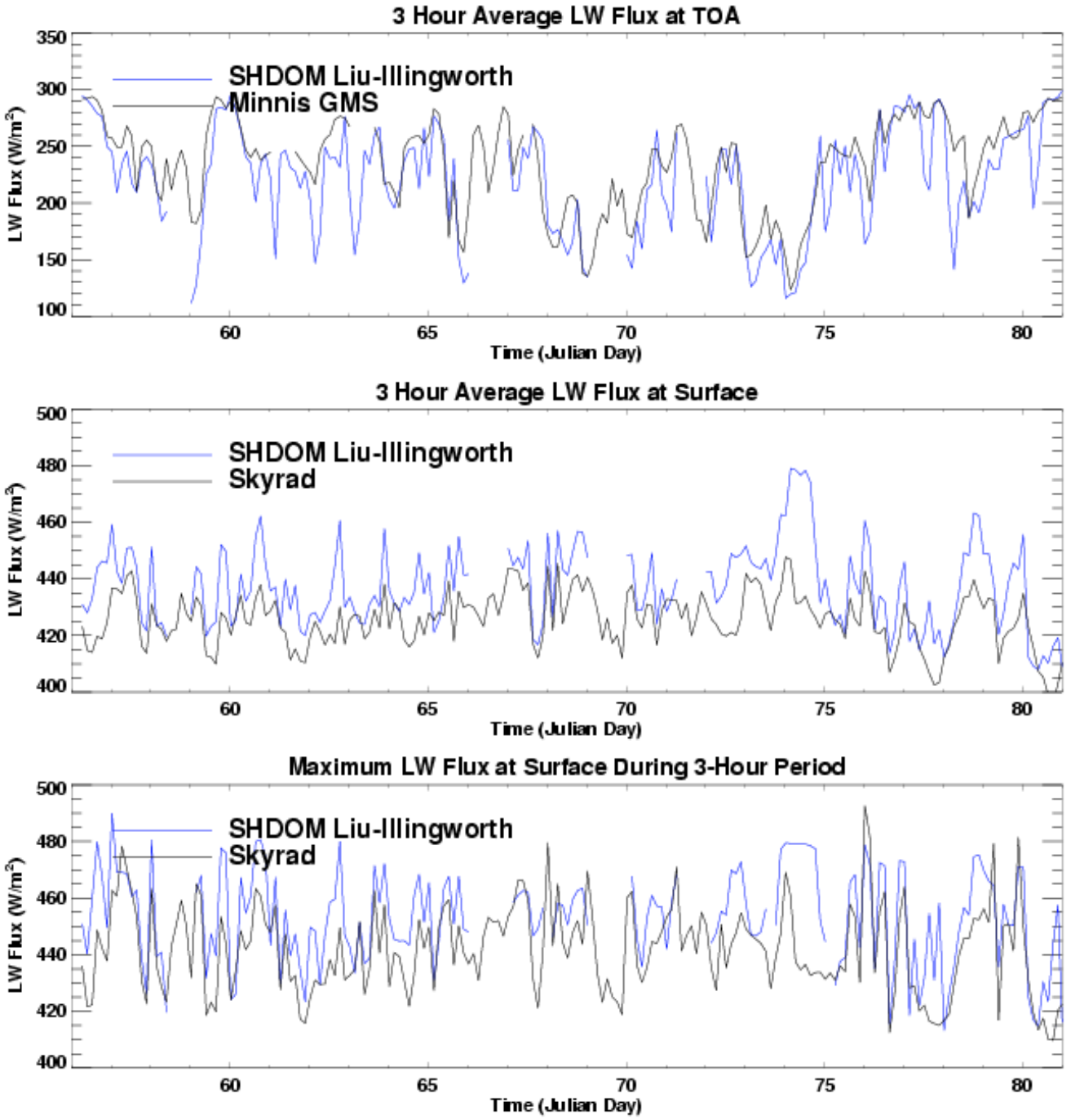

Figure 5. Comparison of observed surface and top of atmosphere longwave fluxes with fluxes calculated from the microbase and associated thermodynamic profiles.

Large Scale Structure in Heating Rate Profile

The condensed water statistics in Figure 2 reveal a distinct vertical structure in cloud properties. This structure should lead to a corresponding vertical structure in radiative heating/cooling due to clouds. To examine this structure, we have calculated the average radiative heating and cooling rates as a function of altitude for the Manus and Nauru study periods. The results of some of these calculations are shown in Figure 6. For Nauru, heating rate profiles for both the clear-sky and all-sky (the averaged cloud product) calculations are shown. All-sky heating rate profiles for Manus are also shown. The clear-sky profile for Manus was very similar to the profile for Nauru. In each plot, five separate profiles are given to separate several physical processes. As seen in the heating rate profiles in Figure 4, radiative fluxes can lead to heating or cooling. Shortwave fluxes only heat the atmosphere but longwave (approximately 4-100 micrometers) can either heat or cool the atmosphere. Cooling is more typical for longwave radiation but heating can occur near the base of clouds. The five plots in each panel are: longwave cooling (negative heating), longwave heating, net longwave heating, shortwave heating, and total heating (the net of all longwave and shortwave effects).

The all-sky profiles are more similar to the clear-sky profiles than we had expected. There are two notable differences for Nauru. First, there is a pronounced longwave effect associated with boundary layer clouds (cooling at cloud top and heating at cloud base). The large magnitude of this feature may reflect the high frequency of boundary layer clouds observed at Nauru due to island contamination. This feature is not observed at Manus. Second, in the clear-sky feature there is no long-wave heating except near and above the tropopause. In the all-sky case, there is significant longwave heating, particularly above 8 km. The effect of this longwave heating is to reduce the net cooling at cirrus altitudes. Thus, at Nauru, cirrus have a net heating effect. A similar set of profiles are observed at Manus but the magnitude of the longwave heating above 8 km is larger and there is also a peak in longwave cooling near 12 km. As observed at Nauru, the net radiative impact of the cirrus at Manus is to warm the cirrus layer.

Local Effects of Radiative Heating Rates

In the previous section, we examined long term averages of the radiative heating rate profiles. These average profiles indicate the large scale impact of radiative heating and can be used to study the feedback of radiative processes on regional dynamics. However, radiative processes are also expected to be important on much shorter time scales, providing feedback to the evolution of clouds.

Radiative heating or cooling can lead to a change in temperature, evaporation or condensation, or vertical motion. In order to better understand the magnitude of the calculated heating rates we have estimated the potential vertical motion that could be induced by this heating. We have estimated the vertical motion by solving the thermodynamic energy equation for vertical velocity. The thermo-dynamic energy equation relates diabatic heating with horizontal advection, adiabatic expansion, and local temperature change (Holton 1979). In solving this equation, we have made several significant assumptions, namely that latent heating and horizontal advection are negligible. The point of this exercise is to illustrate the potential magnitude of radiative heating on vertical motion rather than to suggest that latent heating and horizontal advection of heat are negligible.

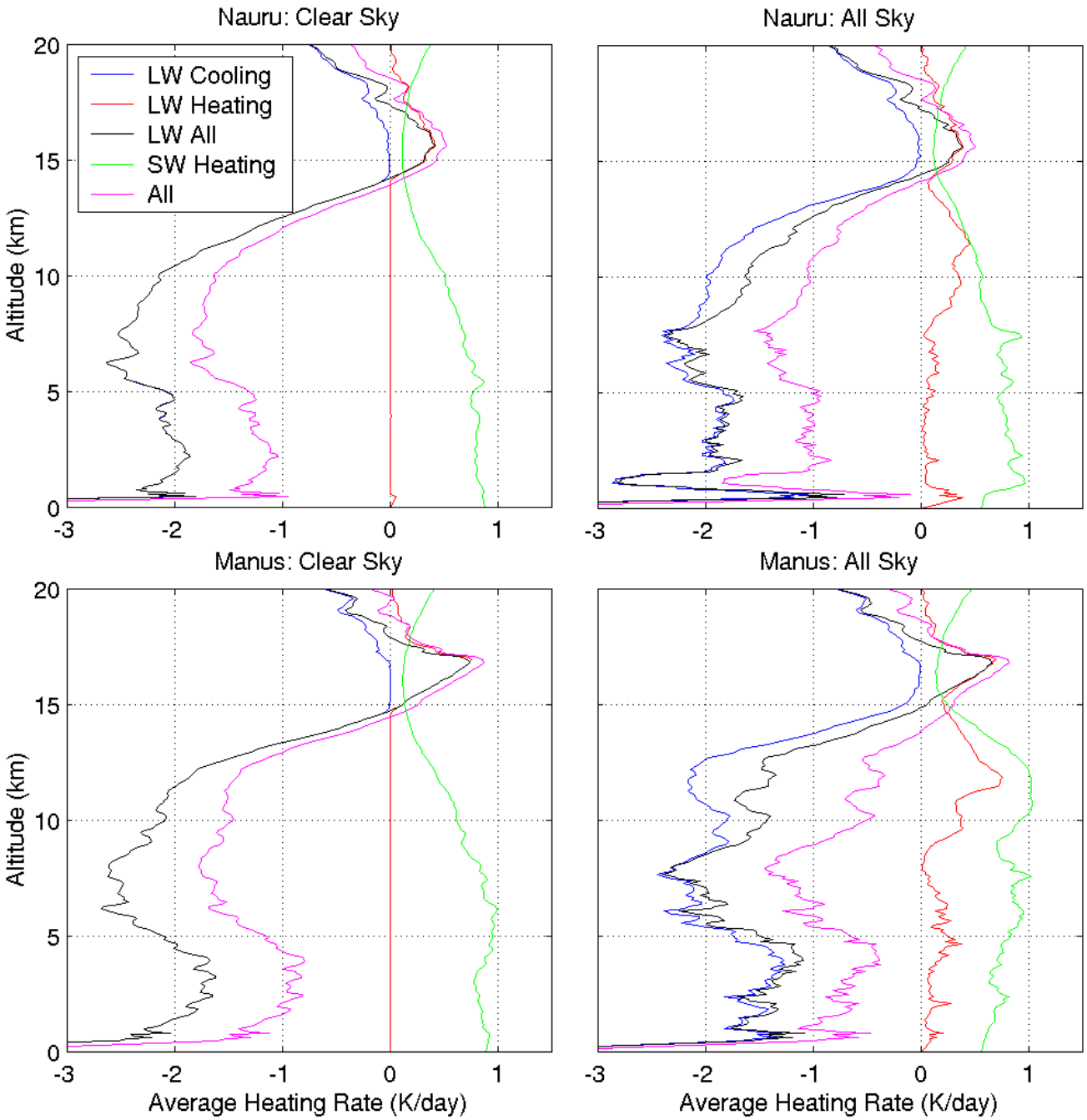

Figure 6. Monthly averaged heating rate profiles for Nauru clear-sky (upper left), Nauru all-sky (upper right), Manus clear-sky (lower left), and Manus all-sky (lower right).

Figures 7 and 8 show the results of these vertical velocity calculations. Figure 7 show the profiles of condensed water, heating rates, and the vertical velocities derived from the thermodynamic energy equation. The color scales have been truncated to bring out patterns rather than absolute amplitudes. The detailed vertical structure is shown in the single time step vertical profile in Figure 8. In this figure, the vertical heating rate and velocity profiles are shown next to the condensed water profile. The peak

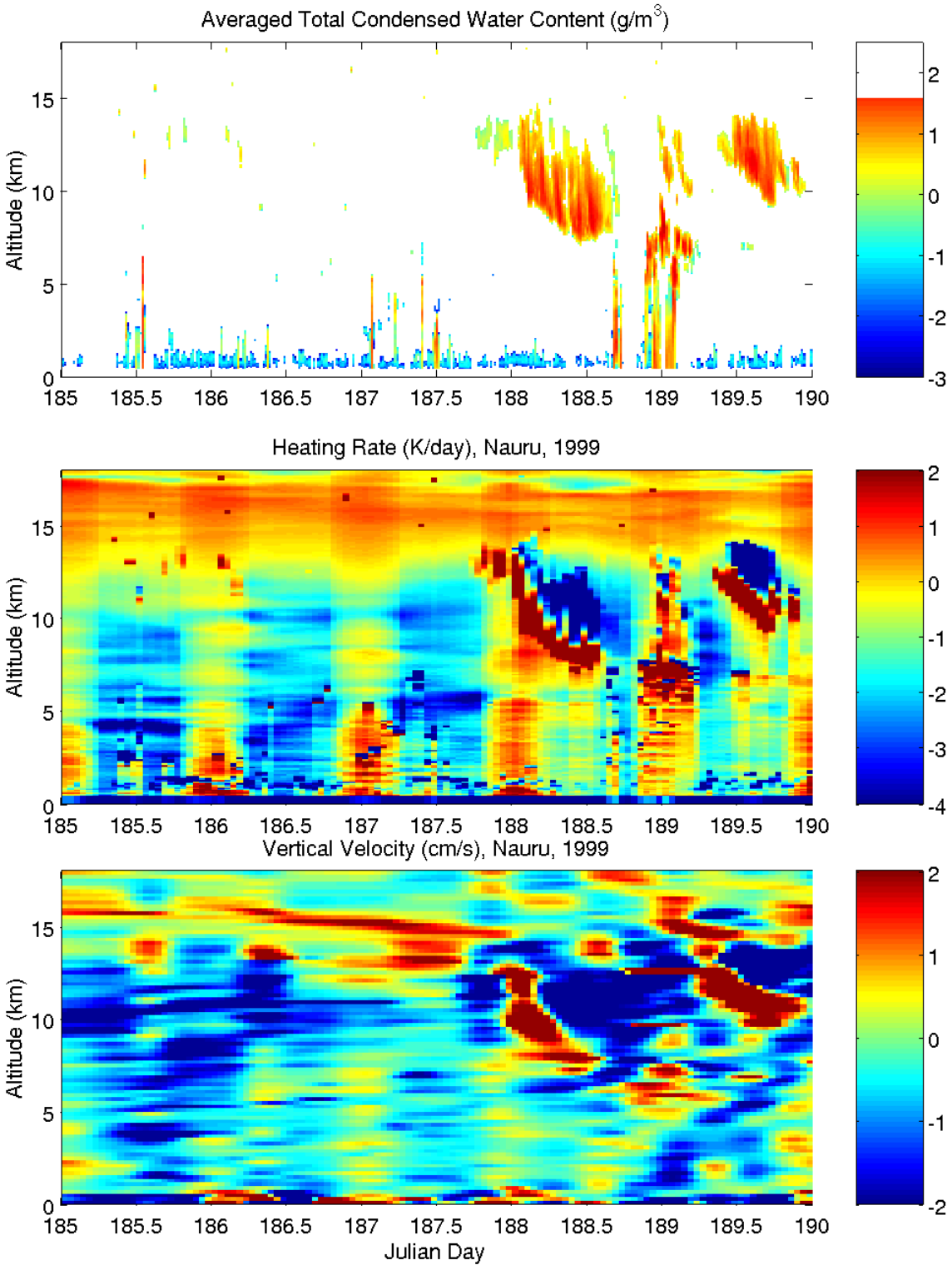

Figure 7. Profiles of condensed water content, radiative heating rate, and vertical velocity. The vertical velocity profiles were derived from the residual of the radiative heating rate and temperature anomalies.

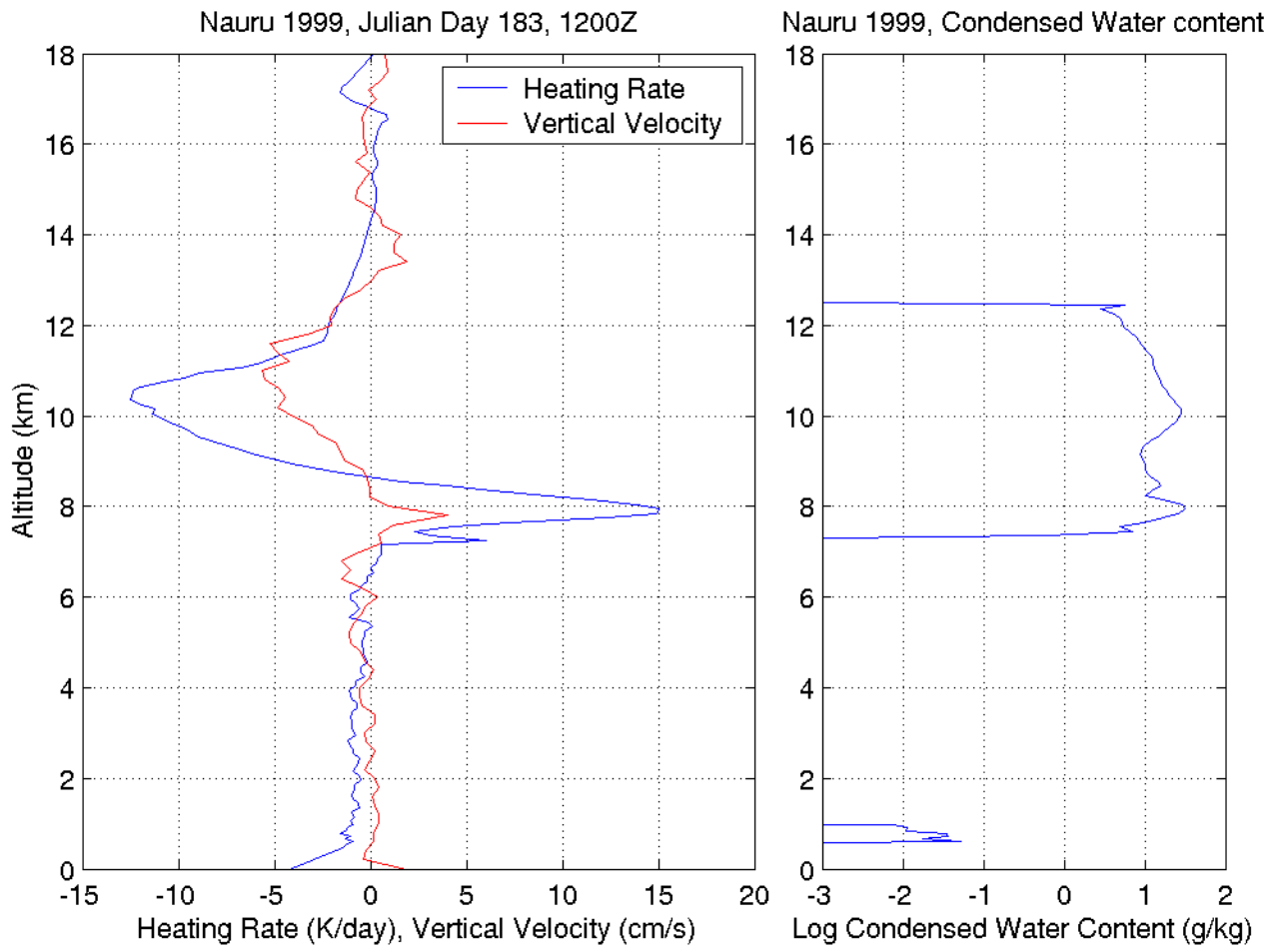

Figure 8. A single profile of condensed water content, radiative heating rate, and vertical velocity. This profile corresponds to 12Z on day 188.

downward velocity calculated for the cirrus layer is 5 cm/s. In the upper panel in Figure 7, the cirrus layer on day 188 is seen to be descending. The slope of this layer is consistent with a descent rate of 5-10 cm/s. This agreement suggests that radiative cooling may play an important role in the evolution of cirrus layers.

Conclusions

Microbase provides a very useful framework for processing and analyzing cloud microphysical properties. While work remains to understand the uncertainties in retrievals applied in this work, we have found a number of interesting features in the microphysical properties produced by microbase as well as in the resulting radiative heating rates. By examining the statistics of cloud properties derived in this study, we observe clear evidence of a tri-modal cloud structure with peaks in the boundary layer (shallow convection), in the upper troposphere (outflow from deep convection), and near 5 km (detrainment at the freezing level). In long term averages of heating rates, we find that the absolute magnitude of effects due to clouds is of the same order or smaller as the effect due to clear skies. The

largest radiative impact due to clouds is seen at the top of the boundary layer (cooling) and between 8-14 km (heating). Radiative processes are also shown to be important on time scales on the order of a day. On these time scales, radiation may play a role in effecting the evolution of cloud layers. Potential vertical velocities associated with radiative heating were calculated by assuming any imbalance between radiative heating and temperature residuals resulted in vertical motion. These calculations result in velocities in cirrus on the same order as observed layer vertical motion.

Acknowledgements

Thanks to Karen Johnson and Mark Miller at Brookhaven National Laboratory for providing the microbase code and for help with its implementation and to the Atmospheric Radiation Measurement program for supporting this work.

Corresponding Author

Jim Mather, Jim.Mather@pnl.gov, 509-375-4533

References

Ackerman, T. P., K. N. Liou, F. P. J. Valero, and L. Pfister, 1988: Heating Rates in Tropical Anvils. *J. Atm. Sci*., **45**, 1606–1623.

Evans, K. F., 1998: The spherical harmonics discrete ordinates method for three-dimensional atmospheric radiative transfer. *J. Atmos. Sci*., **55**, 429–446.

Holton, J. R., 1979: *An Introduction to Dynamic Meteorology*, 2nd edition, Academic Press.

Liu, C. L., and A. J. Illingworth, 1999: Toward more accurate retrievals of ice water content from radar measurements of clouds. *J. Appl. Meteor.*, **39**, 1130–1146.

Miller et al., 2003: ARM Value-Added Cloud Products: Description and Status. In *Proceedings of the Thirteenth Atmospheric Radiation Measurement (ARM) Science Team Meeting*, ARM-CONF-2003. U.S. Department of Energy, Washington, D.C.

Mlawer, E. J., S. J. Taubman, P. D. Brown, M. J. Iacono and S. A. Clough, 1997: RRTM, a validated correlated-k model for the longwave. *J. Geophys. Res.*, **102**, 16,663–16,682.

Nordeen, M. L., D. R. Doelling, P. Minnis, M. M. Khaiyer, A. D. Rapp, and L. Nguyen, 2001: GMS-5 satellite-derived cloud properties over the tropical western Pacific. In *Proceedings of the Eleventh Atmospheric Radiation Measurement (ARM) Science Team Meeting*, ARM-CONF-2001. U.S. Department of Energy, Washington, D.C. Available URL: http://www.arm.gov/publications/proceedings/conf11/abstracts/nordeen-ml.pdf

Yang, P., K. N. Liou, K. Wyser, and D. Mitchell, 2000: Parameterization of the scattering and absorption properties of individual ice crystals. *J. Geophys. Res.*, **105**, 4699–4718.